

## ACCEPTED MANUSCRIPT

This is an early electronic version of an as-received manuscript that has been accepted for publication in the Journal of the Serbian Chemical Society but has not yet been subjected to the editing process and publishing procedure applied by the JSCS Editorial Office.

Please cite this article as A. Amara-Rekkab, *J. Serb. Chem. Soc.* (2024) <https://doi.org/10.2298/JSC230920022A>

This “raw” version of the manuscript is being provided to the authors and readers for their technical service. It must be stressed that the manuscript still has to be subjected to copyediting, typesetting, English grammar and syntax corrections, professional editing and authors’ review of the galley proof before it is published in its final form. Please note that during these publishing processes, many errors may emerge which could affect the final content of the manuscript and all legal disclaimers applied according to the policies of the Journal.





*J. Serb. Chem. Soc.* **00(0)** 1-16 (2024)  
JSCS-12601

## Central composite design (CCD) and artificial neural network-based Levenberg-Marquardt algorithm (ANN-LMA) for the extraction of lanasyn black by cloud point extraction

AFAF AMARA-REKKAB<sup>1,2\*</sup>

<sup>1</sup>Institute of Science and Technology, Department of Hydraulics, University Center of Maghnia, Maghnia, Algeria, <sup>2</sup>Laboratory of Separation and Purification Technologies, Department of Chemistry - Faculty of Sciences, University of Tlemcen, Box 119, 13000, Algeria

(Received 20 September 2023; revised 8 November 2023; accepted 3 March 2024)

**Abstract:** The Lanasyn Black is among the most often used in manufacturing and is challenging to take out during wastewater treatment was acquired in the textile industry. Cloud point extraction was used for their elimination in an aqueous solution. The multivariable process parameters have been independently optimized using central composite design and Levenberg-Marquardt algorithm-based artificial neural network for the highest yield of the extraction of Lanasyn Black via cloud point extraction. The CCD forecasts the output maximum of 97.01% under slightly altered process parameters. Still, the ANN-LMA model predicts the extraction yield (99.98%) using an amount of  $\text{KNO}_3 = 1.04$  g, beginning pH of solution = 8.99, initial of Lanasyn Black 24.57 ppm, and 0.34 W/W of Triton X-100. With coefficients of determination of 0.997 and 0.9777, the most recent empirical verification of the model mentioned above's predictions using CCD and ANN-LMA is determined to be satisfactory.

**Keywords:** dyes; wastewater; extraction; optimisation; surface methodology; neural models; environment.

### INTRODUCTION

Pollutant levels in wastewater from textile manufacturers are typically high. They include up to 1 g/L of the particles and significant levels of organic contaminants in soluble and colloidal forms. In any case, their colour intensity as a function of dilution is one of the most distinctive indicators of textile industry effluent pollution.<sup>1-4</sup> The colour of wastewater is largely attributable owing to the widespread use of organic dyes in the textile industry. During manufacturing, dyes are applied to fibers, textiles, and final goods, depending on the business's expertise. Between 10% and 50% of the pigments used throughout the dying

\* Corresponding author. E-mail: [amarafaf@yahoo.fr](mailto:amarafaf@yahoo.fr)  
<https://doi.org/10.2298/JSC230920022A>

procedure are still present in the technical waste solutions and cleaning water that is produced after cleaning the dyed articles.<sup>5</sup> Because of this, the intensity of color in wastewater from textile businesses that use dyes during the production cycle might approach 1: 1000. The amount of coloring and the level of dilution in the home and industrial wastewater discharged simultaneously. Using green and sustainable technology necessitates the use of alternative processes that utilise fewer organic solvents.<sup>7</sup>

Until now, numerous methods for removing dyes from aqueous solutions, industrial detritus, and polluted water have been reported, including the following: adsorption, electrochemical process, flocculation, membrane filtration, chemical oxidation and biodegradation.<sup>8-10</sup>

Over the past ten years, Cloud point extraction (CPE) is an effective extraction method and has continuously developed.<sup>11,12</sup> CPE has several advantages over conventional pre-treatment methods, including ease of use, increased efficiency, safety, and environmental friendliness.<sup>13</sup> To obtain phase separation from the extraction solution, the solubilization of the surfactant and cloud point phenomena are utilised primarily.<sup>14</sup> Typically, the hydrophilic phase of a surfactant expands in water to produce a long, flexible vermiform micelle. As a result, a tiny volume of the surfactant-rich phase might contain a large amount of the analytes that interact with micellar systems. The analytes move to the inside of the micelles and become securely attached to the hydrophobic groups once the concentration of the surfactant exceeds the micelles' critical point, micelles will form.<sup>15-16</sup> In contrast to the most traditional non-ionic surfactants, Triton X-100 (T100) is a non-ionic surfactant with a distinct structure of the hydrophobic component T100, specifically, features an alkyl-aryl (octyl-phenyl) group as its hydrophobic component instead of an aliphatic tail. It is widely employed in the field of biochemical research as well as in some pharmaceutical formulations and biological system applications.<sup>17</sup>

"Clariant" of Switzerland manufactures the anionic azo dye "Lanasyn Black M-DL," also known as "Lanasyn Black." The dye is one of the most frequently used in manufacturing and is difficult to eliminate during effluent treatment.<sup>5</sup>

Our work's objective focuses on removing Lanasyn Black by cloud point extraction using non-ionic extractant Triton X-100 and using ionic liquid Aliquat 336. A salting-out technique was implemented, which permits the phase separation of surfactants with high cloud points, including TX-100, at room temperature. When combining a nonionic salt with an inorganic salt ( $\text{KNO}_3$ ), the cloud point of a surfactant solution decreases as the salt concentration increases. The reason for this is because the water molecules surrounding the nonionic surfactant exhibit a higher degree of orientation towards the salt anions (such as  $\text{NO}_3^-$ ) even under normal room temperature conditions.<sup>18</sup> The influence of function variables was studied using a Central composite design and artificial neural network based on

Levenberg-Marquardt algorithm. The optimal conditions of the extraction of our dye were determined.

## MATERIALS AND METHODS

### Materials

Complex Textile (Soitex) in Tlemcen, Algeria sells Black Lanasyn ( $C_{38}H_{32}CrN_8O_{10}S_2$ ). Triton X-100 is a non-ionic surfactant with an HLB value of 13.5 and a critical micelle concentration (CMC) of  $3.0 \times 10^{-4}$  M at 25 °C, was employed in this investigation. The  $KNO_3$  99% came from Merck, used to decrease the point cloud temperature to room temperature. Aldrich is the source of Aliquat 336 (tri-capryl-methyl-ammonium chloride  $CH_3N[(CH_2)_7CH_3]_3Cl$ ). Sigma-Aldrich manufactures sodium hydroxide (NaOH) and hydrochloric acid (HCl). Chemopharma provides the ethanol 96% ( $C_2H_6O$ ) needed. To make our solutions, we used distilled water.

### Batch extraction experiments

Every alteration done throughout this work is based on the Triton X-100 and added mass of  $KNO_3$  cloud point extraction of the organic contaminant Black Lanasyn (LN). At room temperature and in graduated tubes, from 1.5 to 4 % of Triton X100 was added to  $Na_2SO_4$  from 0.5 to 1 g, added to 1mL of Aliquat 336 at 0.3 M dissolved in 5 mL of the mother solution of LN from 10 to 20 ppm and then supplemented up to 10 mL with the same solution. The solution's pH ranged from 2.4 to 6.82. The solutions are left to stand for 30 min. Then, centrifuged at 2000 rpm for 10 min, and UV-VISIBLE measures the diluted phase at absorption band  $\lambda_{max} = 570$  nm. The various procedures taken throughout the Black Lanasyn (LN) organic pollutant extraction using cloud point are shown in Fig.1.

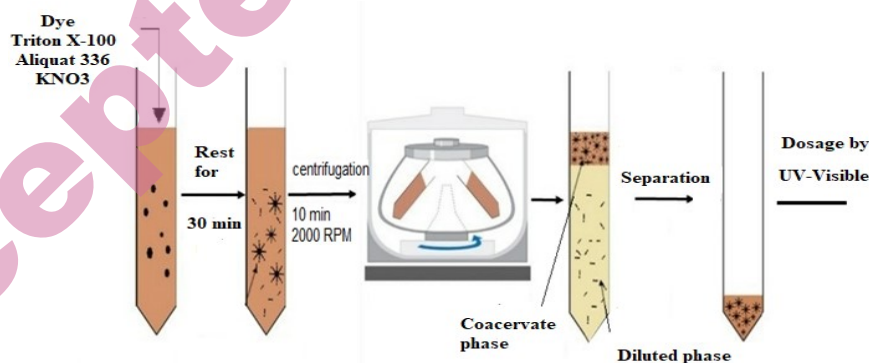


Fig. 1. Schema of the CPE of Lanasyn Black.

Black Lanasyn solutions' UV-Vis absorbance was measured using an SP-UV 200S UV-Visible spectrophotometer. Adwa pH Metre was used to measure pH. The LN removal efficacy (%) was calculated by :<sup>19,20</sup>

$$\text{Removal (\%)} = \frac{C_i - C_e}{C_i} \times 100 \quad (1)$$

where  $C_i$  is the initial concentration and  $C_e$  is the equilibrium concentration of LN.

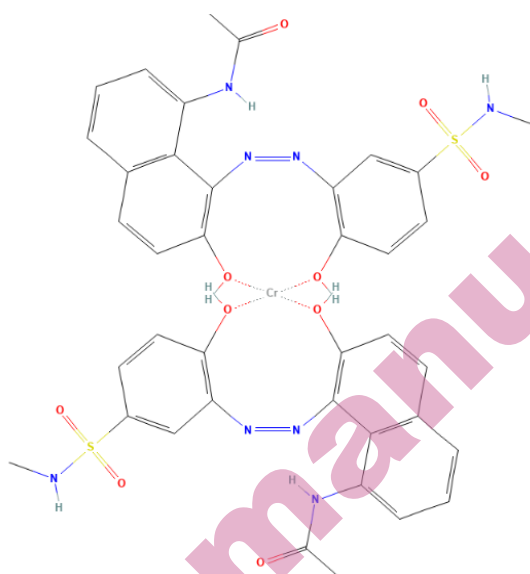


Fig. 2. Chemical structure of the anionic Lanasyne Black dye.

#### Central composite design

The Central composite design (CCD) is the most frequently employed among all multivariate methods. CCD determines how each component affects how the other factors interact. With the least amount of time and effort, this method establishes the system's ideal circumstances. This approach focuses on achieving several specific objectives, the most crucial of which is to enhance the process by identifying the best input.<sup>21</sup>

In this work, CCD was successfully employed to examine the impact of various variables on the effectiveness of Lanasyne Black's extraction by cloud point extraction. Four distinct factors' experimental ranges and levels were selected. Table I lists the mass of  $\text{KNO}_3$  ( $X_1$ ), Triton X-100 ( $X_2$ ), initial pH of the solution ( $X_3$ ), and initial dye concentration ( $X_4$ ). The following equation was used to calculate the results of 31 experimental runs. The following Equation was used to code the factors:<sup>22-24</sup>

$$x_i = \frac{X_i - X_0}{\Delta X} \quad (2)$$

Where  $x_i$ ,  $X_i$ ,  $X_0$ , and  $\Delta X$  are the coded values of the factors, their corresponding real values, the centre point of the real independent variable, and the step between the real variables, respectively.

The multi-regression polynomial (Eq. 3) can be used to represent mathematical representation of connected the independent factor with the outcome:<sup>25-27</sup>

$$y (\%) = A_0 + \sum_{i=1}^k A_i X_i + \sum_{i=1}^k A_{ii} X_i^2 + \sum_{i=1}^k \sum_{j=i+1}^k A_{ij} X_i X_j + \varepsilon \quad (3)$$

As far as they are concerned,  $A_0$  denotes the expected response,  $A_i$ ,  $A_{ii}$ ,  $A_{ij}$  represents the constant coefficient, and  $X_i$ ,  $X_j$  represents the input components in coded values. Finally, it means the overall error. Statistical software Design Expert 13 created the response surface, contour plots, and statistical data analysis.

TABLE I: Summary of CCD Design

level	Experimental factors with their units			
	Mass of KNO <sub>3</sub> (X <sub>1</sub> )	Triton X-100 (X <sub>2</sub> )	pH of the solution (X <sub>3</sub> )	Initial dye concentration (X <sub>4</sub> )
-2	0.25	0.025	0.19	5
-1	0.5	0.15	2.4	10
0	0.75	0.275	4.61	15
1	1	0.4	6.82	20
2	1.25	0.525	9.03	25

*Artificial neural network – Levenberg-Marquardt algorithm (ANN-LMA)*

Artificial neural network simulation is a mathematical instrument. It predicts the linear and nonlinear relationships between multiple inputs and outputs in a complex process. Individually, ANN and CCD can be used to optimise the non-linear process parameters of our dye extraction; however, they are highly interdependent on the input parameters. Due to the presence of beams of highly corresponding elements known as neurons, ANN is regarded as more accurate than CCD.<sup>28-30</sup> Input, hidden, and output layers are the distinct divisions of multiple neurons that comprise the ANN model. Hidden layers, which can have a single or multiple architectures, are the operating units that function as character detectors and introduce nonlinearity into the network. The development of an ANN model is contingent upon multiple phases.<sup>31-33</sup> The phase of learning and the phase of validation. Using previously presented CCD data and the Levenberg-Marquardt feedback algorithm, an ANN model was developed and trained. However, the data points were generated using the second-order polynomial equation of Central composite design. Fig. 3 shows the simple structure of the current ANN-LMA:

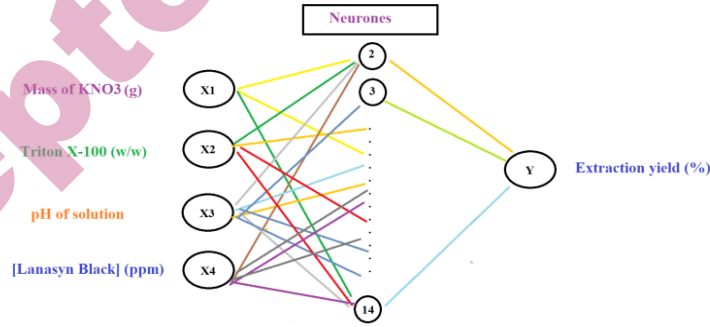


Fig. 3. Proposed modeling by ANN-GA.

As error functions, we used the mean absolute error (MAE), the mean square error (MSE), the root mean squared error (RMSE), and the absolute average deviation (AAD) to evaluate the performance of the ANN model in predicting the dependent variable. It is determined using the following equations:<sup>28</sup>

$$MAE = \left(\frac{1}{n}\right) \sum_{i=1}^n |E_{model} - E_{exp}| \quad (4)$$

$$MSE = \frac{\sum_{i=1}^n (E_{model} - E_{exp})^2}{n} \quad (5)$$

$$\text{ADD (\%)} = 100 \cdot \left( \frac{1}{n} \right) \left( \sum_{i=1}^n \frac{|E_{\text{model}} - E_{\text{exp}}|}{E_{\text{exp}}} \right) \quad (6)$$

$$\text{RMSE} = \sqrt{\frac{\sum_{i=1}^n (E_{\text{model}} - E_{\text{exp}})^2}{n}} \quad (7)$$

## RESULT AND DISCUSSION

### Statistical results

According to the combinations selected using central composite modeling, the experimental matrix shown in Table II comprises 31 experiments. Using this approach, we identified the four elements that were evaluated that were the most critical parameters and the synergic interactions.

The five-level matrix generated by CCD and ANN-LMA with the responses obtained experimentally for the extraction of our dye is shown in Table II. It is clear from the table the extraction yield was obtained around the center of all parameters. The anion of Lanasy Black, negatively charged, reacts in the coacervate phase, Triton X-100 and the ammonium cation of Aliquat 336 form mixed micelles as shown in Fig 4.<sup>34</sup>

On the basis of these findings, the empirical relationships between the response of CCD and selected variables have been determined:

**Extraction yield (%)** = 97,511 - 0,200 Mass of KNO<sub>3</sub> + 1,403 Triton X-100 + 0,766 pH + 0,300 [LN] - 2,618 Mass of KNO<sub>3</sub> \* Mass of KNO<sub>3</sub> - 4,205 Triton X-100 \* Triton X-100 - 1,330 pH\*pH - 2,137 [LN]\* [LN] - 0,261 Mass of KNO<sub>3</sub> \* Triton X-100 - 1,628 Mass of KNO<sub>3</sub> \*pH - 1,162 Mass of KNO<sub>3</sub> \*[LN] + 1,966 Triton X-100 \*pH + 0,382 Triton X-100 \*[LN] + 2,357 pH\*[LN].

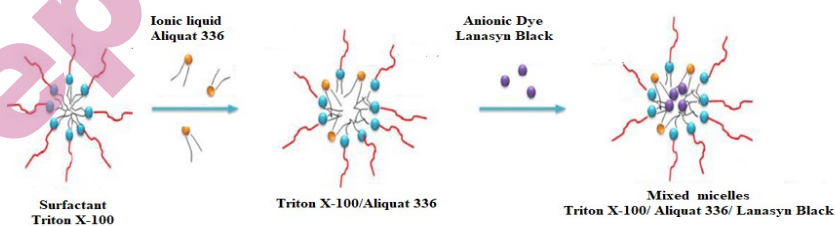


Fig. 4. Lanasy Black dye extraction using combined Triton X-100/Aliquat 336 micelles.

TABLE II: Experimental matrix of experimental data, CCD and ANN-LMA for the extraction of Lanasyn Black

Run order	Mass of KNO <sub>3</sub> (%)	Triton X-100 (W/W)	pH	Lanasyn Black (ppm)	Extraction yield (%)	Predicted value by CCD (%)	Predicted value by ANN (%)
1	-1	-1	-1	-1	88.98	86.6054	88.8945302
2	-1	1	1	-1	90.22	89.2438	90.2931885
3	1	1	-1	1	83.24	84.2225	84.1005084
4	1	1	-1	-1	91.00	89.8971	91.2489692
5	1	-1	1	1	83.60	84.1642	84.4159927
6	1	-1	-1	-1	89.83	92.3075	90.6289325
7	1	-1	1	-1	82.44	81.9387	83.89133
8	0	0	0	0	96.78	97.5114	97.7391311
9	2	0	0	0	88.26	86.6404	89.4786037
10	0	0	0	0	98.02	97.5114	97.7391311
11	-1	-1	1	-1	82.59	82.7492	83.2669267
12	-1	1	-1	-1	84.66	85.2375	83.0878711
13	-1	-1	-1	1	82.30	84.0508	84.4210992
14	0	0	2	0	93.15	93.7221	93.9104141
15	1	-1	-1	1	84.91	85.1054	86.2595135
16	-2	0	0	0	86.18	87.4388	87.6001534
17	0	0	0	0	98.00	97.5114	97.7391311
18	0	0	-2	0	91.59	90.6571	91.4822843
19	0	0	0	0	97.00	97.5114	97.7391311
20	0	2	0	0	82.74	83.4954	83.0456114
21	-1	1	-1	1	84.49	84.2104	84.5912063
22	0	0	0	2	91.28	89.5638	91.6904094
23	-1	-1	1	1	89.30	89.6221	88.7290656
24	1	1	1	1	89.55	91.1438	91.1766252
25	0	0	0	0	98.02	97.5114	97.7391311
26	-1	1	1	1	98.98	97.6442	98.3143374
27	0	-2	0	0	79.00	77.8838	79.963546
28	1	1	1	-1	88.00	87.3908	90.3381571
29	0	0	0	0	97.76	97.5114	97.7391311
30	0	0	0	0	97.00	97.5114	97.7391311
31	0	0	0	-2	87.01	88.3654	89.8871532

To find the significant main and interaction effects of dye extraction parameters, an ANOVA (Table III) was performed.

TABLE III: ANOVA for CCD-Quadratic model

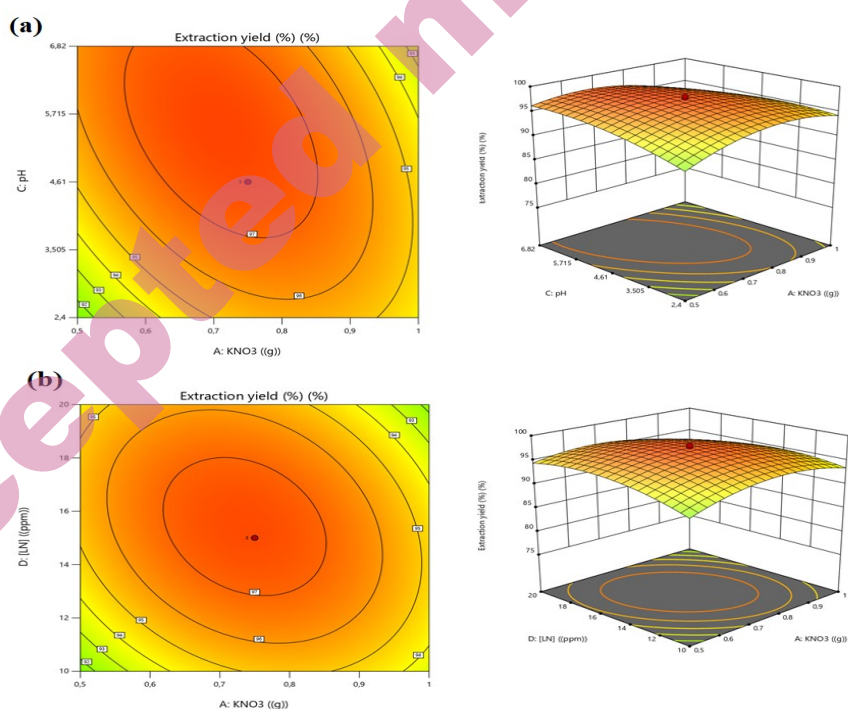
Source	Sum of Squares	df	Mean Square	F-value	p-value	
Model	706.27	14	50.45	16.50	< 0.0001	Significant
A-Mass of KNO <sub>3</sub>	0.9560	1	0.9560	0.3128	0.5863	
B-Triton X-100	47.24	1	47.24	15.45	0.0020	
C-pH	14.09	1	14.09	4.61	0.0529	
D-[Lanasyn Black]	2.15	1	2.15	0.7047	0.4176	
AB	1.09	1	1.09	0.3555	0.5621	
AC	42.41	1	42.41	13.88	0.0029	
AD	21.60	1	21.60	7.07	0.0209	
BC	61.82	1	61.82	20.22	0.0007	
BD	2.33	1	2.33	0.7633	0.3994	
CD	88.88	1	88.88	29.08	0.0002	
A <sup>2</sup>	146.45	1	146.45	47.91	< 0.0001	
B <sup>2</sup>	377.68	1	377.68	123.56	< 0.0001	
C <sup>2</sup>	37.88	1	37.88	12.39	0.0042	
D <sup>2</sup>	97.59	1	97.59	31.93	0.0001	
Residual	36.68	12	3.06			
Lack of Fit	35.83	10	3.58	8.38	0.1113	Not significant
Pure Error	0.8552	2	0.4276			
Cor Total	742.95	26				
			Adeq	R <sup>2</sup>	R <sup>2</sup>	R <sup>2</sup>
Model			Precision	95.06	(adjust)	(predicted)
				15.1637	%	89.30 %
						71.97 %

The Model F-value of 16.50 to  $F_{\text{critic}}(0.05, 14, 12) = 2.65$  indicates that the model is statistically significant. There is only a 0.01% possibility that this large cloud's F-value is caused by noise. P-values less than 0.05 indicate significant model terms. In this particular instance, Triton X-100. Mass of KNO<sub>3</sub>\*pH. Mass of KNO<sub>3</sub>\*[Lanasyn Black]. Triton X-100\*pH. pH\*[Lanasyn Black]. Mass of KNO<sub>3</sub><sup>2</sup>. Triton X-100<sup>2</sup>. pH<sup>2</sup>. [Lanasyn Black]<sup>2</sup> are significant model terms. Values exceeding 0.1000 indicate that the model terms are not statistically significant. The Lack of Fit F-value of 8.38 indicates that the Lack of Fit is not statistically significant in comparison to the pure error  $(0.05, 10, 2) = 19.4$ . Due to noise, there is an 11.13 percent probability that a Lack of Fit F-value will occur in this large cloud. The Predicted R<sup>2</sup> of 0.7197 corresponds reasonably well to the Adjusted R<sup>2</sup> of 0.8930; i.e., the difference is less than 0.2. **Adeq<sub>Precision</sub>** measures the signal-to-noise ratio. Our ratio of 15.164 indicates a sufficient signal. This model can be utilised to navigate the design space.

### Contour plots and response surfaces

Fig. 5 is a graphical representation of the correlations between significant, optimal values and specific output variability by the contour plots and response surface. By possible point extraction, these images aid in understanding and describing the combined impact of the two variables on Lanasyne black extraction.<sup>35</sup> Depending on the contour plot's morphologies, the interaction's significance may be high if the contour plot is elliptical and saddle-shaped, but low if it depicts a circular shape. The maximum response value under the influence of the operational inputs was effectively determined by keeping the remaining pair of factors at their midpoint at the same time.<sup>36</sup>

The elliptical contour diagrams depict the significant impact of interactions between the Mass of  $\text{KNO}_3$ \*pH, Mass of  $\text{KNO}_3$ \*[Lanasyne Black], Triton X-100\*pH, and pH\*[Lanasyne Black]. The maximum extraction yield was achieved at the center level of all parameters, suggesting significance.



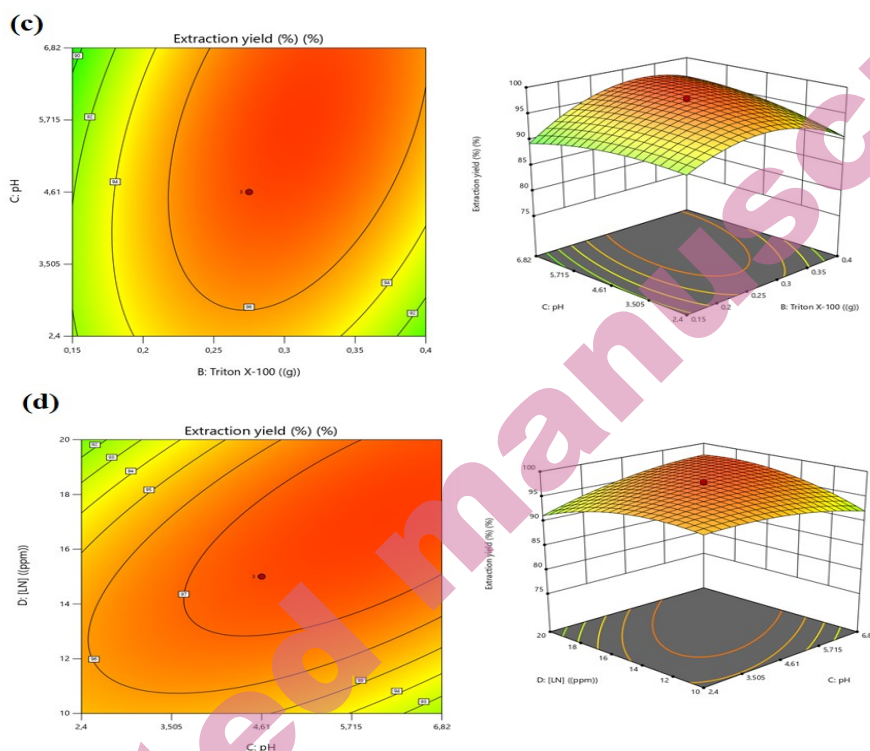


Fig. 5. Contour plots and response surface of the effects: (a) Mass of  $\text{KNO}_3$  and initial pH of the solution; (b) Mass of  $\text{KNO}_3$  and initial concentration of Lanasyne black; (c) Triton X-100 and initial pH of the solution; (d) initial pH of the solution and initial concentration of Lanasyne black on the extraction of Lanasyne black by cloud point extraction.

#### Response optimization

Response optimization was used to optimize the extraction in MINITAB 19.0, and the experiment was run at the specified solution, yielding an extraction rate of 97.87 %, which was extremely close to the predicted value. The mass of  $\text{KNO}_3$  was 1.07575 g, Triton X-100 was 0.368 W/W, the beginning pH of the solution was 9.03, the initial concentration of Black Lanasyne was 22.575 ppm, and this combination produced the highest extraction yield.

#### ANN-LMA modelling

Using a feed-forward back propagation network and the Levenberg-Marquardt algorithm, the ANN-GA model was developed. Three data set subdivisions were generated. Each subset contained 80% of the testing data, 10% of the validation data, and 10% of the network training data. It is important to note that these divisions were wholly arbitrary. Inputs and outputs are immutable elements of the ANN's topology (architecture). Moreover, the number of concealed layers and their respective neurons represent a series of variable elements.

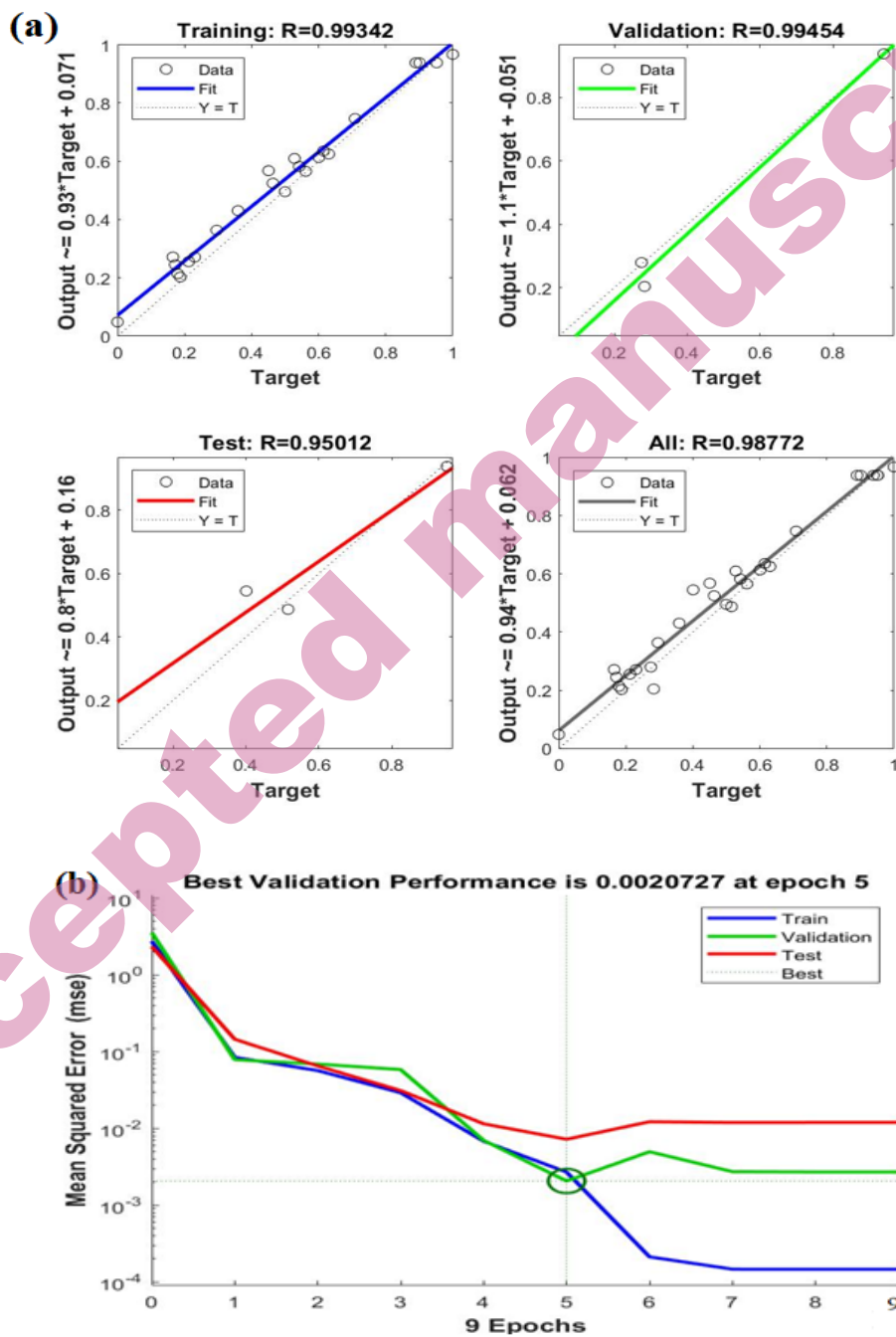


Fig. 6. Regression and performance plots of the ANN-LMA model.

Fig. 6 shows that learning converged after 9 periods with the lowest average square error. Thus, during the ANN iterative learning, the model achieved a maximum R-value of 0.987772 (Fig. 6a) and a minimum MSE value of  $2.0727 \times 10^{-3}$  (Fig.6b) at nine epochs for ten neurons in the hidden layer. Therefore, the best 4-10-1 network architecture is used for process optimization, representing 4 entries in the first layer, 10 hidden neurons, and one upper layer output. The  $R^2$  value close to 1 and a low MSE value indicate that the performance of the developed model is satisfactory and corresponds to the experimental extraction values of the LN per point of disruption.

The reliability of the postulated model for predicting the maximum output data was confirmed while using the optimal points suggesting the ANN<sup>37</sup> ( $\text{KNO}_3$  mass: 1.04 g; beginning pH of solution=8.99, initial of Black Lanasin 24.57 ppm, and 0.34 W/W of Triton X-100). The extraction yield of the experimentally recorded LN was 99.98 % suggesting the suitability and validity of the model. However, the optimum achieved by ANN resulted in an even higher extraction yield than with CCD modelling.<sup>38-41</sup>

*Comparative study between CCD and ANN-LMA*

In order to evaluate the efficacy of the CCD and ANN models, the outputs were compared to the relevant experimental data.

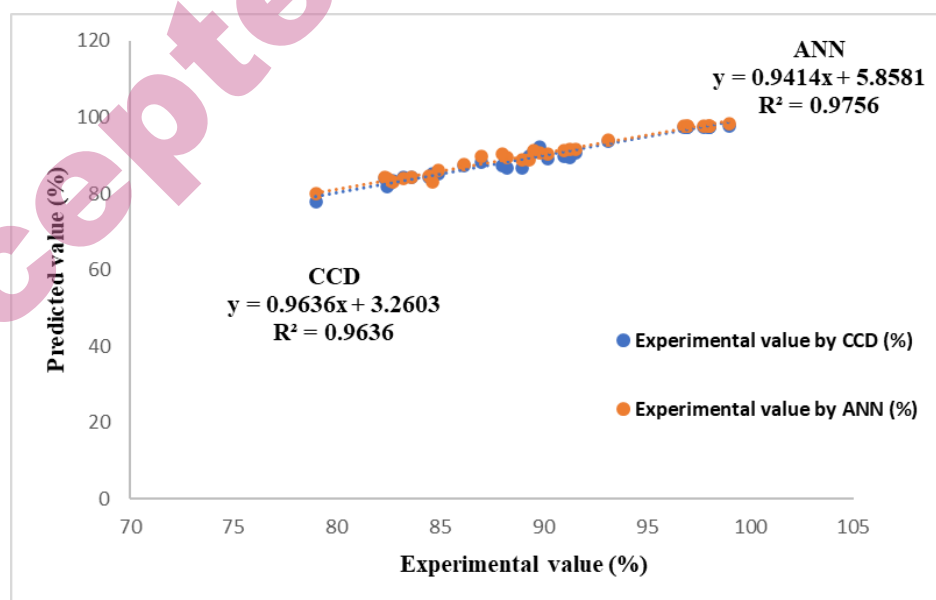


Fig. 7. Comparative parity diagram of experimental and predicted results.

To verify the suitability of the given models, the Black Lanasyn extraction yield predicted by the CCD and ANN models was compared with the experimental results obtained in Table 2. Fig. 7 shows a comparative parity diagram of predicted and experimental results.

The determination coefficient  $R = 0.97498$  for the CCD model and  $R = 0.98772$  for the ANN model shows that the values of the model-based predictions are in perfect accordance with the experimental results.

As a result, the proposed models are well-adapted to data and provide stable responses. However, compared to the RSM model, the ANN model has a higher predictive capacity and accuracy based on the experimental results. The R-value is closer to 1.0.

In addition to the regression coefficient (R), the observed MAE, MSE, AAD, and RMSE values for both models were determined to provide a statistical indication of the accuracy of the model predictions. The MAE, MSE, AAD, and RMSE values for the CCD and ANN models have been calculated and are presented below.

The MAE (0.1203), MSE (0.4488), AAD (0.1363%) and RSME (0.6699) for the CCD model are higher than those (0.0955, 0.2831, 0.1097 % and 0.5321, respectively) for the ANN model. This means the ANN model offers a higher modeling capacity than the CCD model. This result is similar to several researchers.<sup>42,43</sup>

#### CONCLUSION

The Lanasyn black was obtained by the textile sector, and is among of the more frequently used in manufacturing. It is difficult to remove during wastewater treatment. Their removal in an aqueous solution was accomplished by cloud point extraction. For the most significant yield of the extraction of Lanasyn Black using cloud point extraction, the multivariable process parameters have been independently optimized using Central composite design (CCD) and Artificial Neural Network- Levenberg-Marquardt algorithm (ANN-LMA). The ANN-LMA model predicts the extraction yield (99.98%) in optimal conditions. The most recent experimental validation of the model mentioned above's predictions using ANN-LMA and CCD is found to be good, with coefficients of determination of 0.997 and 0.9777, respectively.

*Dedicated to the memory of Professor Mohamed Amine DIDI, who passed away on January 17, 2023. You will never be forgotten, my dear Professor.*

## ИЗВОД

ЦЕНТРАЛНИ КОМПОЗИТНИ ДИЗАЈН (CCD) И LEVENBERG-MARQUARDT АЛГОРИТАМ  
ЗАСНОВАН НА ВЕШТАЧКОЈ НЕУРОНСКОЈ МРЕЖИ (ANN-LMA) ЗА ИЗДВАЈАЊЕ  
ЛАНАСИН ЦРНЕ БОЈЕ ЕКСТРАКЦИЈОМ У ТАЧКИ ЗАМУЋЕЊАAFAF AMARA-REKKAB<sup>1,2</sup>

<sup>1</sup>Institute of Science and Technology, Department of Hydraulics, University Center of Maghnia, Maghnia, Algeria, <sup>2</sup>Laboratory of Separation and Purification Technologies, Department of Chemistry - Faculty of Sciences, University of Tlemcen, Box 119, 13000, Algeria

Ланасин црна боја је међу најчешће коришћеним у производњи, нарочито текстилној индустрији, и тешко је уклонити је током третмана отпадних вода. За њену елиминацију у воденом раствору коришћена је екстракција у тачки замућења. Параметри мултиваријантног процеса су независно оптимизовани коришћењем централног композитног дизајна и вештачке неуронске мреже, засноване на Levenberg-Marquardt алгоритму за највећи принос екстракције Ланасин црне боје у тачки замућења. CCD предвиђа излазни максимум од 97.01%, под благо измењеним параметрима процеса. Ипак, ANN-LMA модел предвиђа принос екстракције од 99.98%, користећи количину KNO<sub>3</sub>=1.04 g, почетни рН раствора 8.99, почетну вредност Ланасин црне боје од 24.57 ppm и 0.34 W/W Тритона X-100. Са коефицијентима детерминације од 0.997 и 0.9777, најновија емпиријска верификација предвиђања модела помоћу CCD и ANN-LMA је одређена као задовољавајућа.

(Примљено 20. септембра 2023; ревидирано 8. новембра 2023; прихваћено 4. марта 2024.)

## REFERENCES

1. D. A. Yaseen, M. Scholz, *Int. J. Environ. Sci. Technol.* **16** (2019) 1193 (<https://doi.org/10.1007/s13762-018-2130-z>)
2. B. K. Nandi, A. Goswami, M. K. Purkait, *Appl. Clay. Sci.* **42** (2009) 583 (<https://doi.org/10.1016/j.clay.2008.03.015>)
3. Krasnoborodko I.G. *Destructive wastewater treatment from dyes*. L: Chemistry, 1988.
4. M. Ghaedi, H. Hossainian, M. Montazerzohori, A. Shokrollahi, F. Shojai pour, M. Soylak, M. K. Purkait, *Desalination*. **281** (2011) 226 (<https://doi.org/10.1016/j.desal.2011.07.068>)
5. V. Geissen, H. Mol, E. Klumpp, G. Umlauf, M. Nadal, M. D. Ploeg, S. E. A. T. M. Van de Zee, C. J. Ritsema, *Int. Soil Water Conserv. Res.* **3** (2015) 57 (<https://doi.org/10.1016/j.iswcr.2015.03.002>)
6. N. E. Djebbari, A. Amara; A. Didi; M. A. Didi., *Scientific Study & Research Chemistry & Chemical Engineering, Biotechnology, Food Industry.* **23** (2022) 333 (<https://pubs.ub.ro/dwnl.php?id=CSCC6202204V04S01A0005>)
7. H. Chandarana, P. Senthil Kumar, M. Srinivasan, M. Anil Kumar, *Chemosphere* **285** (2021) 131480 (<https://doi.org/10.1016/j.chemosphere.2021.131480>)
8. M. K. Dahri, M. R. R. Kooh, L. B.L. Lim, *Alex. Eng. J.* **54** (2015) 1253 (<https://doi.org/10.1016/j.aej.2015.07.005>)
9. E. Brillas, E. Mur, R. Sauleda, L. Sanchez, J. Peral, X. Domenech, J. Casado, *Appl. Catal. B: Environ.* **16** (1998) 31 ([https://doi.org/10.1016/S0926-3373\(97\)00059-3](https://doi.org/10.1016/S0926-3373(97)00059-3))

10. P. Liang, J. Li, X. Yang, *Microchim Acta*. **152** (2005) 47-51 (<https://doi.org/10.1007/s00604-005-0415-7>)
11. D. Snigur, E. A. Azooz, O. Zhukovetska, O. Guzenko, W. Mortada, *TrAC, Trends Anal. Chem.* **164** (2023) 117113 (<https://doi.org/10.1016/j.trac.2023.117113>)
12. R. Halko, I. Hagarová, V. Andruch, *J. Chromatogr. A*. **1701**(2023) 464053 (<https://doi.org/10.1016/j.chroma.2023.464053>)
13. H. S. Ferreira, M. A. Bezerra, S.L.C. Ferreira, *Microchim Acta*. **154** (2006) 163 (<https://doi.org/10.1007/s00604-005-0475-8>)
14. W. R. Melchert, F. R. P. Rocha, *Rev. Anal. Chem.* **35** (2016) 41 (<https://doi.org/10.1515/revac-2015-0022>)
15. J. Yongsheng, W. Le, L. Ruihong, W. Haohao, S. Shuhui, C. Mingzhuo, *ACS Omega* **6** (2021) 13508 (<https://doi.org/10.1021/acsomega.1c01768>)
16. M.N. Jones, *Int. J. Pharm.* **177** (1999) 137 ([https://doi.org/10.1016/s0378-5173\(98\)00345-7](https://doi.org/10.1016/s0378-5173(98)00345-7))
17. A. Amara-Rekkab, M.A. Didi, *Desalin. Water Treat.* **281** (2022) 186 (<https://doi.org/10.5004/dwt.2023.29147>)
18. N. Sato, M. Morin, H. Itabashi, *Talanta* **117** (2013) 376-381 (<https://doi.org/10.1016/j.talanta.2013.08.025>)
19. A. Asfaram, M. Ghaedi, A. Goudarzi, M. Rajabi, *Dalton Trans.***44** (2015) 14707 (<https://doi.org/10.1039/C5DT01504A>)
20. G. Hanrahan, K. Lu, *Crit. Rev. Anal. Chem.* **36** (2006) 141 (<https://doi.org/10.1080/10408340600969478>)
21. M. Boulahbal, M. A. Malouki, M. Canle, Z. Redouane-Salah, S. Devanesan, M. S. AlSalhi, M. Berkani, *Chemosphere* **306** (2022) 135516 (<https://doi.org/10.1016/j.chemosphere.2022.135516>)
22. H. Ucbeyiy, *Fuel. Process. Technol.* **106** (2013) 1 (<https://doi.org/10.1016/j.fuproc.2012.09.020>)
23. G. E. B. Box, W.G. Hunter, J.S. Hunter, *Statistics for Experimenters*, 2 nd edition, Wiley-Interscience, Hoboken, NJ, 1978.
24. T. Mehmood, A. Ahmed, A. Asif, A. M. Sheeraz, M. A. Sandhu, *Food Chem.* **253** (2018) 179 (<https://doi.org/10.1016/j.foodchem.2018.01.136>)
25. S.I.S. Al-Hawary, K. Azhar, S. A. Sherzod, A.K. Kareem, K. A. Alkhuzai, Romero-R.M. Parra, A. H. Amini, T. Alawsi, M. Abosooda, M. Dejaverdi, *Alex. Eng. J.* **74** (2023) 737 (<https://doi.org/10.1016/j.aej.2023.05.066>)
26. K. Behera, H. Meena, S. Chakraborty, B.C. Meikap, *Int. J. Min. Sci. Technol.* **28** (2018) 621 (<https://doi.org/10.1016/j.ijmst.2018.04.014>)
27. M. Maleki-Kakelar A., Aghaeinejad-Meybodi, S. Sanjideh, M. J. Azarhoosh, *Environ. Proc.* **9** (2022) 7 (<https://doi.org/10.1007/s40710-022-00564-0>)
28. P. Mondal, A. K. Sadhukhan, A. Ganguly, P. Gupta, *3 Biotech* **11** (2021) 28 (<https://doi.org/10.1007/s13205-020-02553-2>)
29. N. Teslić, N. Bojanić, D. Rakić, A. Takači, Z. Zeković, A. Fišteš, M. Bodroža-Solarov, B. Pavlič, *Chem. Eng. Process.* **143** (2019) 107634 (<https://doi.org/10.1016/j.ccep.2019.107634>)
30. B. Jiang, F. Zhang, Y. Sun, X. Zhou, J. Dong, L. Zhang, *J. Taiwan Inst. Chem. Eng.* **45** (2014) 2217 (<https://doi.org/10.1016/j.jtice.2014.03.020>)
31. A. Çelekli, H. Bozkurt, F. Geyik, *Bioresour. Technol.* **129** (2013) 396 (<https://doi.org/10.1016/j.biortech.2012.11.085>)

32. A. Smaali, M. Berkani, F. Merouane, V.T. Le, Y. Vasseghian, N. Rahim, M. Kouachi, *Chemosphere* **266** (2021) 129158 (<https://doi.org/10.1016/j.chemosphere.2020.129158>)
33. K. Oukebdane, R. Semmoud, M.A. Didi, *Desalin. Water Treat.* **247** (2022) 272 (<https://doi.org/10.5004/dwt.2022.28039>)
34. M. Berkani, M. Bouhelassa, M. K. Bouchareb, *Arab. J. Chem.* **12** (2019) 3054 (<https://doi.org/10.1016/j.arabjc.2015.07.004>)
35. D. Bas, I. Boya, *J. Food Eng.* **78** (2007) 836 (<https://doi.org/10.1016/j.jfoodeng.2005.11.024>)
36. M. Pravitha, M. R. Manikantan, V. Ajesh Kumar, S. Beegum, R. Pandiselvam, *LWT.* **146** (2021) 111441 (<https://doi.org/10.1016/j.lwt.2021.111441>)
37. J. Han, M. Kamber, J. Pei, *Data Mining: Concepts and Techniques*, 3<sup>rd</sup> Ed., Morgan Kaufmann, 2012.
38. E. Bello, T. Ogedengbe, M. Khumbulani, I. Daniyan, *Procedia CIRP* **89** (2020) 59 (<https://doi.org/10.1016/j.procir.2020.05.119>)
39. R. Pandiselvam, M. R. Manikantan, S. Sunoj, S. Sreejith, S. Beegum, *J. Food Process Eng.* **42** (2019) e12981 (<https://doi.org/10.1111/jfpe.12981>)
40. S. Youssefi, Z. Emam-Djomeh, S. M. Mousavi, *Drying Technology* **27** (2009) 910 (<https://doi.org/10.1080/07373930902988247>)
41. V. Ajesh Kumar, S. Prem Prakash, M. Pravitha, H. Muzaffar, M. Shukadev, V. Prithviraj, V. Deepak Kumar, *Food Pack. Shelf Life* **31** (2022) 100778 (<https://doi.org/10.1016/j.fpsl.2021.100778>)
42. A. J. Sisi, A. Khataee, M. Fathinia, B. Vahid, Y. Orooji, *J. Mol. Liq.* **316** (2020) 113801 (<https://doi.org/10.1016/j.molliq.2020.113801>)
43. Z. Jun, C. Leland, S. Dongyi, W. Y. Zhan, *Appl. Energy.* **345** (2023) 121373 (<https://doi.org/10.1016/j.apenergy.2023.121373>).